Ultrastrong, Foldable, and Highly Conductive Carbon Nanotube Film

Jiangtao Di,[†,‡,⊥] Dongmei Hu,[†,⊥] Hongyuan Chen,[†,‡] Zhenzhong Yong,[†] Minghai Chen,[†] Zhihai Feng,[†] Yuntian Zhu,[§] and Qingwen Li[†,*]

[†]Key Laboratory of Nanodevices and Applications, Suzhou Institute of Nano-tech and Nano-bionics, Chinese Academy of Sciences, Suzhou, 215123, China, [‡]Graduate University of Chinese Academy of Sciences, Beijing 100049, China, and [§]Department of Materials Science and Engineering, North Carolina State University, Raleigh, North Carolina 27695, United States . [⊥]These authors contributed equally to this work.

ABSTRACT

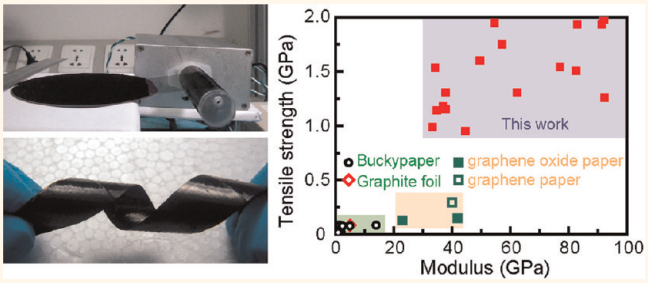

Preparation of strong, flexible, and multifunctional carbon-based films has attracted considerable interest not only in fundamental research areas but also for industrial applications. We report a binder-free, ultrastrong, and foldable carbon nanotube (CNT) film using aligned few-walled nanotube sheets drawn from spinnable nanotube arrays. The film exhibits tensile strengths up to ~2 GPa and a Young's modulus up to ~90 GPa, which is markedly superior to other types of carbon-based films reported, including commercial graphite foils, buckypapers, and graphene-related papers. The film can bear severe bending (even being folded) and shows good structure integrity and negligible change in electric conductivity. The unique structure of the CNT film (good nanotube alignment, high packing density) provides the film with direct and efficient transport paths for electricity. As a flexible charge collector, it favors a magnesium oxide coating to exhibit high charge/discharge rate stability and an excellent electrochemical capacitance close to its theoretical value.

KEYWORDS: carbon nanotube · film · tensile strength · alignment · bending · charge collector

Graphitic carbon-based films have been used in various applications such as engineering materials, electronics, electrochemical electrodes, electromagnetic shielding, packing, and gaskets, due to their unique physiochemical properties.[1−3] A long-standing focus is to develop such film materials with tunable microscale structures and novel macroscale mechanical and electrical conducting properties. Conventional graphite foils are fabricated by pressing exfoliated graphite flakes. The tensile strength of such foils is attributed to the surface roughness of the flakes and is typically in the range 2−12 MPa,[4,5] which is not strong enough for flexible applications. Moreover, graphite foils fracture easily under bending.

Carbon nanotubes (CNTs), consisting of single or multiple rolled graphene layers, possess excellent anisotropic mechanical properties[6] and can even fully recover from severe bending or compressing.[7,8] Tensile strength values for individual nanotubes are experimentally measured as high as 100−200 GPa, and modulus values are ~1 TPa.[9−12] Moreover, CNTs show ballistic conduction behavior for electricity and heat.[13,14] These extraordinary properties have motivated considerable interest in fabricating macroscopic CNT films (buckypapers) for real applications.[15] Although improved mechanical strength up to about 80 MPa has been reported for CNT films compared with graphite foils,[16−18] it is still several orders of magnitude lower than the strength of individual nanotubes. Similar to graphite foils, CNT films crack upon bending or compressing, which limits their applications.

Currently, methods for the preparation of CNT films can be conveniently categorized into wet chemistry and direct growth approaches. The wet chemistry approach, widely used, includes vacuum filtration,[19−21] layer-by-layer (LBL) assembly,[22] solution spraying,[23] spin coating,[24] and draw-down rod coating.[25] In normal cases, CNTs undergo purification to remove impurities (*e.g.*, catalysts and amorphous carbon), dispersion, and deposition into paper-like films in this approach. It can be applied to various carbon nanomaterials such as CNTs and graphene oxide and provides large room for chemical modification of these carbon nanomaterials. However, the CNT films obtained by this approach commonly have poor mechanical

* Address correspondence to qwli2007@sinano.ac.cn.

Received for review March 25, 2012 and accepted May 16, 2012.

Published online May 16, 2012
10.1021/nn301321j

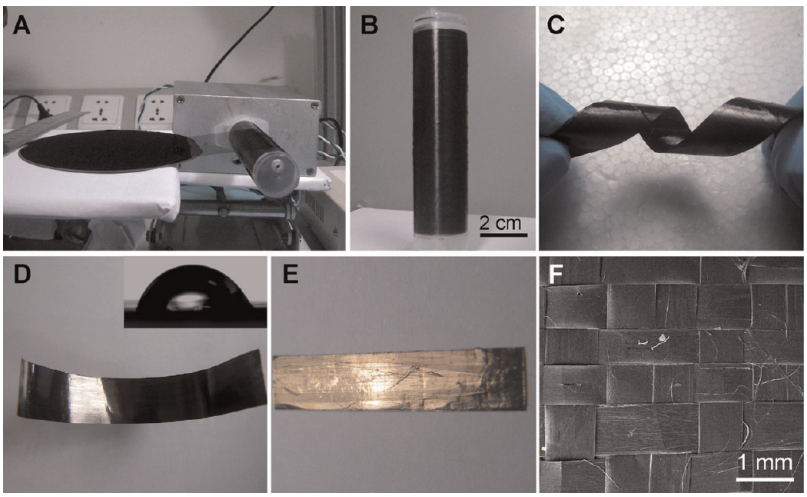

Figure 1. (A) Setup for the preparation of the aligned CNT film. A CNT sheet from a spinnable nanotube array on a 4 in. silicon wafer was continuously wound on a rotating spindle and collected. (B) As-prepared CNT film on a spindle. (C) Flexible CNT film strip. (D) Photographs of a shining CNT strip and (E) strip coated with a 12 nm gold layer. Inset in (D) is the shape of a water droplet on the strip. (F) SEM image of a woven fabric consisting of CNT strips.

strength, and the nanotubes are disorderly aligned in the films. More importantly, during the purification and dispersion process, the native structures of nanotubes are damaged by truncating the nanotubes and inducing many surface defects, which are detrimental to their mechanical and electrical properties. Alternatively, the direct growth approach can avoid such problems. CNT films can be directly and continuously collected downstream of flowing gases that contain carbon source and floating catalyst particles passing through a hot furnace.[26,27] This method is well known for its promising mass production at low cost.[28,29] Unfortunately, the CNTs are randomly aligned in the films. As an alternative, the vertically aligned nanotube array (forest or carpet) that is directly grown on a predeposited catalyst film shows high purity, since the catalyst film is very thin (few nanometers), and most of it stays on the substrate due to the base growth mode.[30] Pure and dense buckypapers can be easily prepared by pushing down the vertical nanotubes in one direction and peeling them off the substrate.[31−33] The nanotubes are tightly aligned in the pushing direction, allowing the buckypaper to outperform most of the vacuum-filtrated buckypapers in terms of mechanical flexibility and thermal and electrical conductance.[31] However, the size of the buckypaper is limited by the substrate wafer, and the mechanical strength of the buckypaper is still low.

In contrast to the mentioned approaches, spinnable CNT arrays offer much flexibility to fabricate various novel carbon forms in a dry state at room temperature.[34] For example, an aligned CNT sheet can be drawn readily from such arrays and shows many promising applications.[35,36] A combination of the drawing process with twisting on the nanotube sheets yields strong and lightweight CNT fibers.[37,38] A method was developed to prepare anisotropic CNT films by LBL stacking of the nanotube sheets.[39] Herein, we report a CNT film fabricated by the solid-state LBL assembly of aligned few-walled CNT sheets that draw from highly spinnable nanotube arrays. Compared with the LBL assembly of positively and negatively charged CNTs,[22] this solid assembly method does not introduce chemical treatment to CNTs and CNT contact with each other through physical interactions such as van der Waals forces. The film is robust, having a tensile strength of 1−2 GPa and exhibiting good structure stability under severe bending and folding. Moreover, it shows anisotropic electrical conductivity and can provide a direct path for charges when used as electrodes for electrochemical cells.

RESULTS AND DISCUSSION

Figure 1A shows the setup for preparation of the CNT film. An aligned and transparent CNT sheet was drawn in the solid state from a spinnable nanotube array and then continuously wound onto a rotating spindle layer by layer to produce a seamless film roll (Figure 1B). The spinnable nanotube array was grown at 750 °C by catalytic chemical vapor deposition using ethylene as carbon source and Fe (1 nm)/Al_2O_3 (10 nm) on a silicon substrate as catalyst (see Experimental Section).[40] A nanotube array with a length of 1 cm can be continuously converted into a 10 m long nanotube sheet at a drawing rate of 1 m/min. The thickness of the CNT film depends on the number of windings, and the width of the film is determined by the initial width of the nanotube sheet. After being taken off the spindle, the seamless CNT film was cut into strips with various widths by a sharp knife. The strips are robust and highly flexible, as shown in Figure 1C. We notice that the as-prepared CNT film appears black, while it becomes shiny after being treated with ethanol (Figure 1D), similar to highly

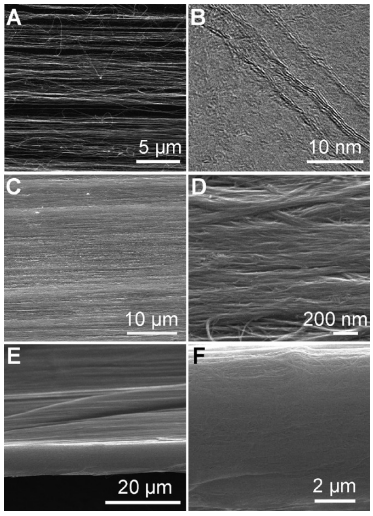

Figure 2. Morphology of an aligned CNT film. (A) SEM image of an as-drawn CNT sheet for the film fabrication. (B) TEM image of CNTs in the sheet. SEM images of the top surface of a densified CNT film at low (C) and high resolution (D), and (E, F) cross section of the CNT film parallel to the nanotube alignment at low (E) and high resolution (F).

ordered pyrolytic graphite (HOPG). The surface property of the film even changes from hydrophobic to somewhat hydrophilic, as indicated by the water contact angle, which decreased from 129° on the original CNT sheet to 73° on the densified film (Figure 1D, and Figure S1 in the Supporting Information). This indicates that a smooth surface consisting of closely packed nanotubes is formed, which may enable the CNT film to act as a suitable scaffold for fabricating cheap and flexible electrodes by depositing a continuous layer of noble metals (*e.g.*, Au, Pt). A CNT film coated with a 12 nm thick Au layer is shown in Figure 1E. The Au/CNT film is highly conductive (<1 ohm/sq) and bendable, with stable electrical conductivity. Fabricating architectures using such CNT films for flexible electrical circuits, electrochemical electrodes, high-strength composites, *etc.*, is achievable. As an example, we wove a textile fabric using some millimeter-wide CNT strips by hand, and its scanning electron microscopy (SEM) image is shown in Figure 1F.

Figure 2A shows a SEM image of the aligned nanotube sheet. The CNTs are self-assembled into small fibrils and align parallel to the drawing direction. The thickness of the sheet is about 50−100 nm. Transmission electron microscopy (TEM) shows that the CNTs in the sheet are few-walled and have small diameters (Figure 2B). Over 95% of the nanotubes have 2−3 graphene walls with a nanotube diameter distribution in a range from 4 to 6 nm, as shown by the statistics on 70 nanotubes (see Figure S2 in the Supporting Information). The surface morphology of the as-prepared CNT films (without densification) is similar to that of the initial CNT sheet; that is, CNTs being spaced by tens of nanometer-wide gaps (see Figure S3 in the Supporting Information). These gaps can not only trap most of incident light, rendering the film low reflectance,[41] but also provide paths for solutions or gases to penetrate into the film to densify it. We used ethanol to shrink the as-prepared CNT film during or after winding. The density of the film increased from 0.6 to 0.9 g cm^{-3} after the solvent densification. It is much higher than that for the films obtained by pressing of vertical CNT forests,[31,32] but still lower than that for the graphite foils due to the hollow structure of nanotubes. SEM images at different magnification reveal that the CNTs are closely packed into a dense assembly and become further straightened after densification, with the gaps disappearing (Figure 2C, D). The nanotube alignment was further confirmed by a polarized Raman spectrum of the film (see Figure S4 in the Supporting Information).[42] High-quality organization of CNTs during the winding process can also be confirmed from the side image of the CNT film parallel to the nanotube alignment (Figure 2E, F).

Figure 3A compares the mechanical parameters including tensile strength and Young's modulus (measured along the nanotube alignment) of our aligned CNT films to the dates collected from the reported carbon-based films including buckypaper, graphene oxide paper, graphene paper, and graphite foil. We plot dates obtained from more than 20 samples. Most of them show tensile strengths above 1.1 GPa, though the modulus shows relatively large variations. The maximal tensile strength (∼2.0 GPa) and Young's modulus (∼90 GPa) of our CNT films are ∼10−20 times and ∼20 times, respectively, higher than those for the previously reported buckypapers[16,18,39,43−46] and also much stronger than the graphene oxide paper,[47,48] graphene paper,[49] and graphite foils.[4,50] We observed that the mechanical parameters are even comparable with the CNT fibers spun from the same array.[51] The data information in Figure 3A is detailed in Table S1 in the Supporting Information. When normalized to the film's density (0.9 g cm^{-1}), the specific tensile strength of our CNT films is much greater than that for aluminum foil (483 MPa, density: 2.8 g cm^{-3}) and high-strength steel (AISI 4130 steel, σ: 1110 MPa, 7.85 g cm^{-3}) and comparable with the value for the rigid carbon fiber laminate (1600−2000 MPa, density: 1.75 g cm^{-3}). To the best of our knowledge, this is the strongest pure CNT film ever reported.

Figure 3B shows representative stress−strain curves for the as-prepared and the densified CNT films. The as-prepared CNT films with a thickness of 8 μm have an average tensile strength of 0.5 GPa and modulus of 13.6 GPa (green). Significant improvements on the tensile strength and modulus have been achieved for the densified films: a tensile strength of 1.5 GPa and a modulus of 66.8 GPa (red). Compared with the as-prepared film, the ultimate tensile strains become smaller for the

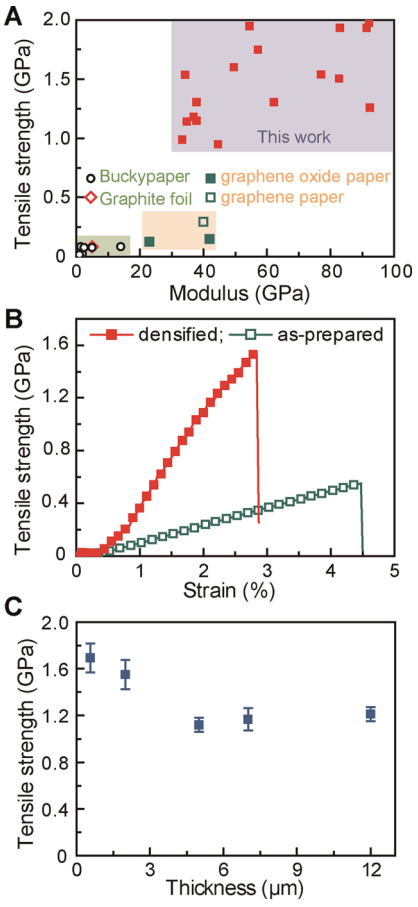

Figure 3. Mechanical behavior of CNT films. (A) Comparison of our CNT films with previously reported buckypapers, graphite foil, and graphene papers in terms of tensile strength and modulus. (B) Representative stress–strain curves for the as-prepared (green) and densified CNT papers (red). (C) Tensile strength as a function of the paper's thickness; each data point was averaged from those of 5 or 6 samples, and the error bars represent the standard error.

densified CNT film, which is about 2.7%. This corresponds with the increased modulus. The work of extension to fracture (toughness) is 17.0 MJ m^{-3} for the densified film, slightly higher than that of the as-prepared film (11.9 MJ m^{-3}). When normalized to density, their toughness is comparable, that is, 18.9 J/g for the densified film and 19.8 J/g for the as-prepared film, respectively. These values are nearly 100 times higher than the buckypapers[16,18,39,43–46] and the graphene oxide paper.[47] It is reasonable that thin films have better mechanical parameters than thick films, as the defects or voids formed in the thin films are less than that in thick films. Bearing this in mind, we investigated the relationship between the thickness and the tensile strength of our CNT films. Although a slight decrease in tensile strength is observed as the thickness increased from 0.5 to 12 μm, most of the CNT films maintained a tensile strength of 1.1–1.6 GPa (Figure 3C). This makes us believe that our films with varying thickness have very consistent structure.

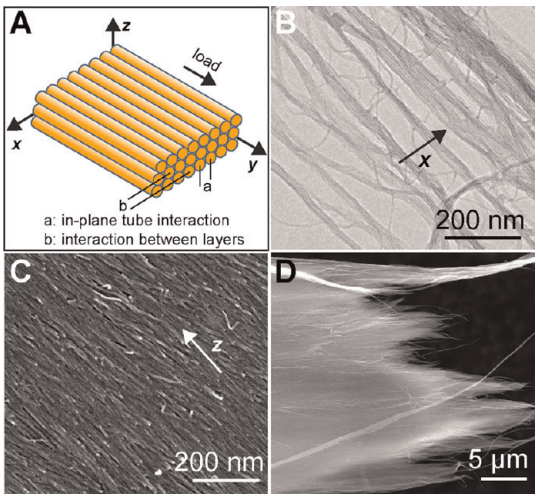

Figure 4. (A) Schematic diagram showing intertube interactions in a CNT film in the *x* axis direction (a, in-plane tube interaction) and in the *z* axis direction (b, interaction between the nanotube layers, the thickness direction) when load is applied in the *y* axis direction. (B) TEM showing fibrils consisting of closely packed nanotubes in an aligned nanotube sheet. The arrow points to the corresponding *x* axis direction in part A. (C) Cross section image of a densified CNT film perpendicular to the nanotube alignment at high resolution; the arrow points in the thickness direction of the CNT film (*z* axis direction). (D) SEM image of the fracture of a CNT film.

The mechanical strength of CNT films is mainly derived from interactions between CNTs, which includes van der Waals force and nanotube entanglement.[52] As a qualitative description, we schematically show the structure of our CNT film in Figure 4A. The intertube interactions mainly exist in two directions: the *x* axis direction (a, in-plane tube interaction in a single nanotube sheet) and the *z* axis direction (b, the thickness direction: interaction between the nanotube layers) when load is applied on the *y* axis direction. The CNTs in the film are typically ~220 μm in length, as determined by the height of spinnable arrays, and they prefer to stick to each other to form small fibrils (Figure 4B). Therefore, strong tube–tube interactions in the *x* axis direction are effectively guaranteed by the long tube contact lengths, favoring most of the nanotubes participating in load bearing.[52,53] During the winding process, the nanotube sheet stacks layer by layer, with nanotubes being aligned in the load direction. After the alcohol densification, the nanotubes are closely packed in the thickness direction, as shown in Figure 4C, a high-resolution SEM image of the cross section of a densified CNT film perpendicular to the nanotube alignment. The high packing density can achieve a large contact area between the nanotubes, and thus the van der Waals force or interfriction gets enhanced in the thickness direction. This is consistent with the comparison results in Figure 3B. For the as-prepared CNT film without densification, the nanotube packing is loose (see Figure S3 in the Supporting Information).

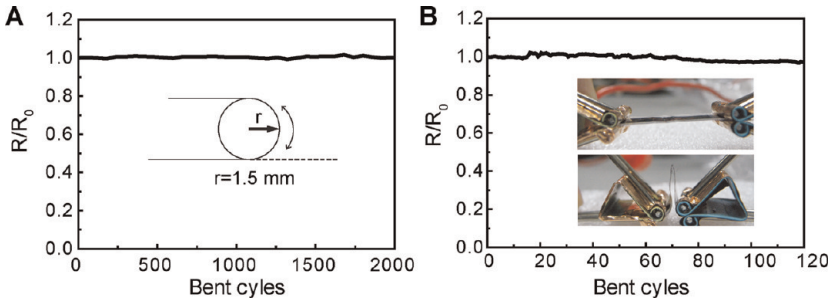

Figure 5. Resistance change of a 6 μm thick CNT film with bending test: (A) after the film was bent to a 1.5 mm radius more than 2000 times; (B) after the film was folded and unfolded many times. Inset in (B) shows the unfolded (above) and folded film (below).

Slippage between the nanotubes occurs easily, which leads to a relatively low mechanical strength and modulus (see the green curve in Figure 3B). The tube−tube joints, which connect CNTs into a continuous sheet, are randomly distributed in the films, and they get pressed during the winding and solution densification. When stretched, the CNTs tend to slip at the joints, resulting in the rough fracture surface after the rupture of the CNT film (Figure 4D). Fracture of individual nanotubes may coexist with the nanotube slipping in our film as previously observed for CNT bundles or fibers.[12,38] These unique features integrated in our films effectively transfer the load to individual nanotubes in the film, achieving high mechanical performance. In contrast, buckypapers prepared by the wet chemistry approach consist of randomly aligned short nanotubes, and the nanotubes are connected only by weak crossings.[54] When stretched, the random nanotubes tend to rearrange in the load direction, and simultaneous slippage occurs between them, which gives rise to the observed poor mechanical properties. Binders or chemical linkages thus were used to prevent the nanotube from sliding, resulting in a strong CNT composite.[55−57] A noteworthy advance for our CNT films is that they are free from binders.

It is worth mentioning that not all CNT films produced by this solid-state assembly can achieve such superior mechanical performances. For example, Zhang *et al*. reported a tensile strength of 232.5 MPa for a CNT film containing 18 layers of nanotube sheets,[35] and Inoue Yoku reported an aligned CNT film having a tensile strength of 80 MPa and Young's modulus of 1 GPa.[39] We recently reported a tensile strength of 420 MPa for a CNT film.[58] Comparison of the nanostructures for different CNTs reveals that the tube diameter is more closely related with the film's tensile strength (see Table S2 in the Supporting Information). The observation is consistent with the results we previously reported for CNT fibers spun from different CNT arrays.[51] Considering that the outermost walls of CNTs play a dominate role in load transfer,[9] large contact areas between CNTs (high packing density) are of great importance for CNT films or fibers to achieve high strength. Small-diameter CNTs are superior because they have fewer crystalline defects, fewer walls, and a large contact area in a unit volume compared to the nanotubes with large diameters. For the growth of small-diameter CNTs, an alumina buffer layer was introduced between a catalytic Fe film and Si substrate, as the alumina layer can effectively retard the aggregation of the catalytic particles, thus favoring the formation of dense small-diameter catalytic particles on the substrate.[59] Additional attention should be paid to the quality (or spinnability) of the few-walled CNT arrays. Superior mechanical performance can be readily obtained when nanotube sheets can be continuously and uniformly drawn from CNT arrays (this kind of array has good spinnability). If the nanotube sheet becomes narrow or branched during the drawing process, the obtained CNT films commonly have a relatively low modulus and tensile strength.

Besides their superior mechanical properties, our CNT films show excellent mechanical flexibility and structure integrity during bending. We applied a very small voltage (0.1 mV) on the two sides of a 6 μm thick CNT film strip along the nanotube alignment and recorded the current passing through the film during a bending test. The resistance calculated from the voltage and the current showed negligible change after the film was bent to a radius of 1.5 mm 2000 times (Figure 5A). Impressively, even after the film was folded and unfolded 180° over 100 times, the resistance did not show an observable increase (Figure 5B). Shear stress is applied on the film during the bending test. The stress is not strong enough to break down the nanotubes, but can make the nanotubes slip in their laminate to accommodate the extension of the outer surface of the film. The extension is closely related with the normal strain (ε), which can be expressed as $\varepsilon = 0.5t/r$, where t is the thickness of the film and r is the radius of curvature. Thus, it is important for the nanotubes to be long enough to withstand the slippage to rupture of CNT films upon bending (Figure 6A, long nanotubes), or the CNT films could crack easily upon bending, as indicated by a CNT film consisting ~10 μm

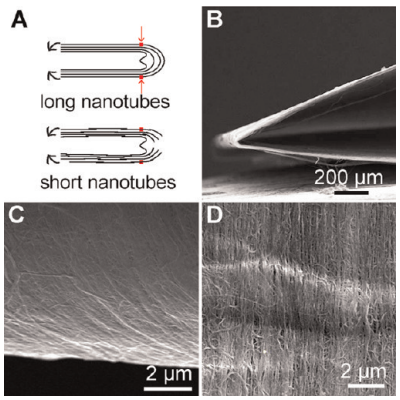

Figure 6. Morphology of a folded CNT film. (A) Schematics illustrating the collapse behaviors of CNT films consisting of long and short nanotubes under bending. (B) SEM image of the folded CNT film; a crease can be clearly seen. (C) Outer side and (D) inner side of the crease on the CNT film.

long random multiwalled carbon nanotubes (Figure 6A, short nanotubes, and Figure S5 in the Supporting Information). As shown previously, the length of the CNTs in our films is about 220 μm. It is easy for such long nanotubes to bridge the elongation caused by the bending stress (shear stress). As shown in Figure 6B, a 6 μm thick aligned CNT strip was folded and a crease was formed. The nanotubes are continuously aligned across the crease at both the outer (Figure 6C) and the inner sides (Figure 6D) of the strip.

The electrical conductivity of our pure CNT film along the nanotube alignment at room temperature is about 35 000 S/m using the four-probe method, higher than the functionalized few-walled nanotube mat reported recently[18] and the random nanotube films prepared using the CNTs from our spinnable arrays (~5500 S/m). Therefore, the unique structure of our CNT film can provide not only excellent mechanical performance but also direct and efficient transport paths for electricity. Compared to the metal foils that are commonly used for charge collectors in electrochemical cells, *e.g.*, lithium ion batteries and supercapacitors, the CNT film is more stable in various solutions and, thus, more suitable for charge collector application. Moreover, the robustness of our CNT film (strong but nonbrittle) can facilitate the fabrication or assembly of electrochemical cells compared with other kinds of buckypapers. As a demonstration, magnesium oxide (MnO_x) was electrochemically deposited on a CNT film, producing a flexible CNT/MnO_x composite electrode. Figure 7A shows the cyclic voltammogram (CV) of a CNT and the composite film from 0 to 1 V *versus* SCE at a scan rate of 100 mV s^{-1} measured in 1 M Na_2SO_4 aqueous solution. A symmetrical rectangular pattern is observed in the CV curve for the composite film, which indicates the film's good capacitive behavior. It is clear that the magnesium oxide coating makes a major contribution to the capacitance of the composite film, as the CNT film shows very low

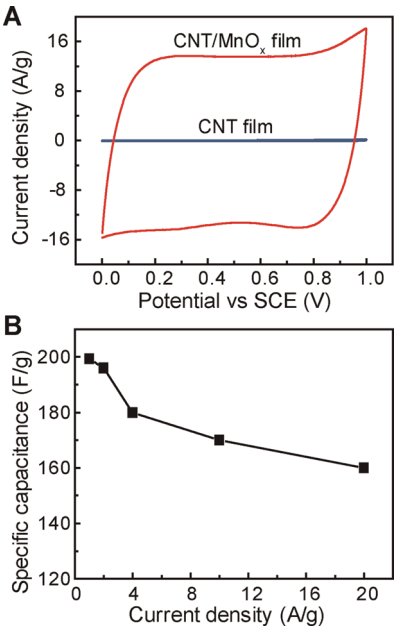

Figure 7. CNT/MnO_x composite film acting as a supercapacitor. (A) Cyclic votammograms of a CNT strip and a composite strip at a scan rate of 100 mV s^{-1} in 1 M Na_2SO_4. (B) Specific capacitances of the composite film at different current density.

electrochemical capacitive activity, as indicated by the small integrated area in its CV curve. The low capacitance of the CNT film further shines light on the film's high packing density. We calculated the specific capacitances at different charging/discharging current density from the galvanostatic charge/discharge curves (see Figure S6 in the Supporting Information) for the composite film, and the results are shown in Figure 7B. The specific capacitance is 199.4 F g^{-1} at a current density of 1 A g^{-1}. With the current density increasing to 20 A g^{-1}, the composite electrode can even maintain 80% capacitance, showing high stability and good rate performance. It is worth mentioning that the capacitance values are obtained based on the mass of the composite electrode. When calculated based on mass of the magnesium oxide layer, the specific capacitance can even reach 1176 F g^{-1} (corresponding to 199.4 F g^{-1} at 1 A g^{-1}), approaching the theoretical capacitance of magnesium oxide.[60,61] Such high capacitance performance is derived from the excellent electrical conductivity of our aligned CNT strip that provides fast charge transport paths for the magnesium oxide coatings.

CONCLUSIONS

We have fabricated ultrastrong, fold-crack-free CNT films by solid-state layer-by-layer assembly of few-walled CNT sheets. Such high-performance CNT films possess four essential features of CNTs: good alignment, long length, small diameter (few walls), and high packing density. Due to the unique structure, the films are very promising for many advanced applications, such as strong composites, heat-conducting foils, and

battery electrodes. Moreover, considering the easy manipulation and scalability, we believe that this method can shed new light on the fabrication of novel carbon-based functional materials.

EXPERIMENTAL SECTION

Growth of Spinnable CNT Arrays. CNT arrays were synthesized in a 5 in. quartz tube at 750 °C by chemical vapor deposition. The catalyst is prepared by in turn depositing an alumina layer (30 nm) and an iron layer (1 nm) on a silicon substrate with thermal oxide by electron-beam evaporation technique. Argon with 6% hydrogen and pure ethylene were used as the forming gas and the carbon source, respectively. The total flow rate of gases was set at 1.5 L/min.

Assembly of the CNT Films. A CNT sheet was drawn from one side of a spinnable array using a blade and further attached on a spindle that was covered by a 40 μm thick polytetrafluoroethylene (PTFE) film. A small angle (5−10°) was kept between the nanotube sheet and the array substrate during the drawing. The winding rate was set at ~1 cm s^{-1}. Ethanol was sprayed onto the nanotubes during or after the winding process. When the winding was finished, the obtained CNT film was put in a drier at 80 °C overnight to remove ethanol. The CNT film together with the PTFE film was taken off the spindle, followed by carefully peeling off the CNT film from the PTFE film.

Characterization. The samples were characterized by scanning electron microscopy (SEM, FEI Quanta 400 FEG, and Hitachi S-4800 HR-FESEM) and high-resolution transmission electron microscopy (HRTEM, FEI Tecnai G2 F20 S-Twin, 200 kV).

Mechanical Test. The films were cut into 15 mm long strips with a width of ~1 mm, which was precisely measured by an optical microscope. The thicknesses of the strips were measured by SEM. Mechanical testing was performed on a testing machine (Instron 3365) with a load cell of 100 N at a displacement rate of 1 mm/min.

Electrochemical Measurement. The electrochemical measurements were performed on a CHI 660C electrochemical workstation. Magnesium oxide was electrochemically deposited on a CNT strip using a constant current method in an aqueous solution containing 0.6 M $MnSO_4$ and 0.8 M H_2SO_4. A three-electrode configuration was used for the cyclic voltammetry and the constant current charge discharge behavior, using the CNT/MnO_x composite as the working electrode, a saturated calomel electrode (SCE) as the reference electrode, and a Pt wire as the counter electrode, respectively. The electrolyte is 1 M Na_2SO_4 solution. Cyclic voltammetry was measured in the potential range between 0 and 1 V *versus* SCE at room temperature at a scan rate of 100 mV s^{-1}.

Conflict of Interest: The authors declare no competing financial interest.

Acknowledgment. This work was supported by the State Key Program of National Natural Science of China (Grant No. 10834004), the National Basic Research Program of China (2011CB605802), the National Key Basic Research Program of China (No. 2011CB932600-G), and the National Basic Research Program of China (2010CB934700).

Supporting Information Available: Figures S1−S5 and Tables S1 and S2. This material is available free of charge via the Internet at http://pubs.acs.org.

REFERENCES AND NOTES

1. Jorio, A.; Dresselhaus, G.; Dresselhaus, M. S. *Carbon Nanotubes: Advanced Topics in the Synthesis, Structure Properties and Applications*; Springer Verlag: Berlin, 2008; Vol. 111.
2. Geim, A. K. Graphene: Status and Prospects. *Science* **2009**, *324*, 1530–1534.
3. Chung, D. D. L. Flexible Graphite for Gasketing, Adsorption, Electromagnetic Interference Shielding, Vibration Damping, Electrochemical Applications, and Stress Sensing. *J. Mater. Eng. Perform.* **2000**, *9*, 161–163.
4. Dowell, M.; Howard, R. Tensile and Compressive Properties of Flexible Graphite Foils. *Carbon* **1986**, *24*, 311–323.
5. Leng, Y.; Gu, J.; Cao, W.; Zhang, T. Y. Influences of Density and Flake Size on the Mechanical Properties of Flexible Graphite. *Carbon* **1998**, *36*, 875–881.
6. Baughman, R. H.; Zakhidov, A. A.; de Heer, W. A. Carbon Nanotubes--the Route toward Applications. *Science* **2002**, *297*, 787–792.
7. Iijima, S.; Brabec, C.; Maiti, A.; Bernholc, J. Structural Flexibility of Carbon Nanotubes. *J. Chem. Phys.* **1996**, *104*, 2089–2092.
8. Cao, A.; Dickrell, P. L.; Sawyer, W. G.; Ghasemi-Nejhad, M. N.; Ajayan, P. M. Super-Compressible Foamlike Carbon Nanotube Films. *Science* **2005**, *310*, 1307–1310.
9. Yu, M.-F.; Lourie, O.; Dyer, M. J.; Moloni, K.; Kelly, T. F.; Ruoff, R. S. Strength and Breaking Mechanism of Multiwalled Carbon Nanotubes under Tensile Load. *Science* **2000**, *287*, 637–640.
10. Peng, B.; Locascio, M.; Zapol, P.; Li, S.; Mielke, S. L.; Schatz, G. C.; Espinosa, H. D. Measurements of near-Ultimate Strength for Multiwalled Carbon Nanotubes and Irradiation-Induced Crosslinking Improvements. *Nat. Nanotechnol.* **2008**, *3*, 626–631.
11. Zhang, R.; Wen, Q.; Qian, W.; Su, D. S.; Zhang, Q.; Wei, F. Superstrong Ultralong Carbon Nanotubes for Mechanical Energy Storage. *Adv. Mater.* **2011**, *23*, 3387–3391.
12. Yu, M. F.; Files, B. S.; Arepalli, S.; Ruoff, R. S. Tensile Loading of Ropes of Single Wall Carbon Nanotubes and Their Mechanical Properties. *Phys. Rev. Lett.* **2000**, *84*, 5552–5555.
13. Javey, A.; Guo, J.; Wang, Q.; Lundstrom, M.; Dai, H. J. Ballistic Carbon Nanotube Field-Effect Transistors. *Nature* **2003**, *424*, 654–657.
14. Mingo, N.; Broido, D. Carbon Nanotube Ballistic Thermal Conductance and Its Limits. *Phys. Rev. Lett.* **2005**, *95*, 96105.
15. Liu, L.; Ma, W.; Zhang, Z. Macroscopic Carbon Nanotube Assemblies: Preparation, Properties, and Potential Applications. *Small* **2011**, *7*, 1504–1520.
16. Zhang, X. F.; Sreekumar, T. V.; Liu, T.; Kumar, S. Properties and Structure of Nitric Acid Oxidized Single Wall Carbon Nanotube Films. *J. Phys. Chem. B* **2004**, *108*, 16435–16440.
17. Baughman, R. H.; Cui, C.; Zakhidov, A. A.; Iqbal, Z.; Barisci, J. N.; Spinks, G. M.; Wallace, G. G.; Mazzoldi, A.; De Rossi, D.; Rinzler, A. G.; *et al.* Carbon Nanotube Actuators. *Science* **1999**, *284*, 1340–1344.
18. Kumar, N. A.; Jeon, I. Y.; Sohn, G. J.; Jain, R.; Kumar, S.; Baek, J. B. Highly Conducting and Flexible Few-Walled Carbon Nanotube Thin Film. *ACS Nano* **2011**, *5*, 2324–2331.
19. Liu, J.; Rinzler, A. G.; Dai, H. J.; Hafner, J. H.; Bradley, R. K.; Boul, P. J.; Lu, A.; Iverson, T.; Shelimov, K.; Huffman, C. B.; *et al.* Fullerene Pipes. *Science* **1998**, *280*, 1253–1256.
20. Wu, Z.; Chen, Z.; Du, X.; Logan, J. M.; Sippel, J.; Nikolou, M.; Kamaras, K.; Reynolds, J. R.; Tanner, D. B.; Hebard, A. F.; *et al.* Transparent, Conductive Carbon Nanotube Films. *Science* **2004**, *305*, 1273–1276.
21. Endo, M.; Muramatsu, H.; Hayashi, T.; Kim, Y. A.; Terrones, M.; Dresselhaus, M. S. Nanotechnology: "Buckypaper" from Coaxial Nanotubes. *Nature* **2005**, *433*, 476–476.
22. Lee, S. W.; Kim, B. S.; Chen, S.; Shao-Horn, Y.; Hammond, P. T. Layer-by-Layer Assembly of All Carbon Nanotube Ultrathin Films for Electrochemical Applications. *J. Am. Chem. Soc.* **2009**, *131*, 671–679.
23. Liu, Q.; Fujigaya, T.; Cheng, H. M.; Nakashima, N. Free-Standing Highly Conductive Transparent Ultrathin Single-Walled Carbon Nanotube Films. *J. Am. Chem. Soc.* **2010**, *132*, 16581–16586.

24. Jo, J. W.; Jung, J. W.; Lee, J. U.; Jo, W. H. Fabrication of Highly Conductive and Transparent Thin Films from Single-Walled Carbon Nanotubes Using a New Non-Ionic Surfactant Via Spin Coating. *ACS Nano* **2010**, *4*, 5382–5388.
25. Dan, B.; Irvin, G. C.; Pasquali, M. Continuous and Scalable Fabrication of Transparent Conducting Carbon Nanotube Films. *ACS Nano* **2009**, *3*, 835–843.
26. Nasibulin, A. G.; Kaskela, A.; Mustonen, K.; Anisimov, A. S.; Ruiz, V.; Kivisto, S.; Rackauskas, S.; Timmermans, M. Y.; Pudas, M.; Aitchison, B.; *et al.* Multifunctional Free-Standing Single-Walled Carbon Nanotube Films. *ACS Nano* **2011**, *5*, 3214–3221.
27. Ma, W. J.; Song, L.; Yang, R.; Zhang, T. H.; Zhao, Y. C.; Sun, L. F.; Ren, Y.; Liu, D. F.; Liu, L. F.; Shen, J.; *et al.* Directly Synthesized Strong, Highly Conducting, Transparent Single-Walled Carbon Nanotube Films. *Nano Lett.* **2007**, *7*, 2307–2311.
28. Cheng, H.; Li, F.; Sun, X.; Brown, S.; Pimenta, M.; Marucci, A.; Dresselhaus, G.; Dresselhaus, M. Bulk Morphology and Diameter Distribution of Single-Walled Carbon Nanotubes Synthesized by Catalytic Decomposition of Hydrocarbons. *Chem. Phys. Lett.* **1998**, *289*, 602–610.
29. Zhu, H.; Xu, C.; Wu, D.; Wei, B.; Vajtai, R.; Ajayan, P. M. Direct Synthesis of Long Single-Walled Carbon Nanotube Strands. *Science* **2002**, *296*, 884.
30. Liu, L.; Fan, S. Isotope Labeling of Carbon Nanotubes and Formation of 12c−13c Nanotube Junctions. *J. Am. Chem. Soc.* **2001**, *123*, 11502–11503.
31. Wang, D.; Song, P. C.; Liu, C. H.; Wu, W.; Fan, S. S. Highly Oriented Carbon Nanotube Papers Made of Aligned Carbon Nanotubes. *Nanotechnology* **2008**, *19*, 075609.
32. Pint, C. L.; Xu, Y. Q.; Pasquali, M.; Hauge, R. H. Formation of Highly Dense Aligned Ribbons and Transparent Films of Single-Walled Carbon Nanotubes Directly from Carpets. *ACS Nano* **2008**, *2*, 1871–1878.
33. Pint, C. L.; Xu, Y. Q.; Moghazy, S.; Cherukuri, T.; Alvarez, N. T.; Haroz, E. H.; Mahzooni, S.; Doorn, S. K.; Kono, J.; Pasquali, M. Dry Contact Transfer Printing of Aligned Carbon Nanotube Patterns and Characterization of Their Optical Properties for Diameter Distribution and Alignment. *ACS Nano* **2010**, *4*, 1131–1145.
34. Jiang, K. L.; Li, Q. Q.; Fan, S. S. Nanotechnology: Spinning Continuous Carbon Nanotube Yarns−Carbon Nanotubes Weave Their Way into a Range of Imaginative Macroscopic Applications. *Nature* **2002**, *419*, 801–801.
35. Zhang, M.; Fang, S.; Zakhidov, A. A.; Lee, S. B.; Aliev, A. E.; Williams, C. D.; Atkinson, K. R.; Baughman, R. H. Strong, Transparent, Multifunctional, Carbon Nanotube Sheets. *Science* **2005**, *309*, 1215–1219.
36. Jiang, K.; Wang, J.; Li, Q.; Liu, L.; Liu, C.; Fan, S. Superaligned Carbon Nanotube Arrays, Films, and Yarns: A Road to Applications. *Adv. Mater.* **2011**, *23*, 1154–1161.
37. Zhang, M.; Atkinson, K. R.; Baughman, R. H. Multifunctional Carbon Nanotube Yarns by Downsizing an Ancient Technology. *Science* **2004**, *306*, 1358–1361.
38. Zhang, X. F.; Li, Q. W.; Holesinger, T. G.; Arendt, P. N.; Huang, J. Y.; Kirven, P. D.; Clapp, T. G.; DePaula, R. F.; Liao, X. Z.; Zhao, Y. H.; *et al.* Ultrastrong, Stiff, and Lightweight Carbon-Nanotube Fibers. *Adv. Mater.* **2007**, *19*, 4198–4201.
39. Inoue, Y.; Suzuki, Y.; Minami, Y.; Muramatsu, J.; Shimamura, Y.; Suzuki, K.; Ghemes, A.; Okada, M.; Sakakibara, S.; Mimura, H.; *et al.* Anisotropic Carbon Nanotube Papers Fabricated from Multiwalled Carbon Nanotube Webs. *Carbon* **2011**, *49*, 2437–2443.
40. Li, Q. W.; Zhang, X. F.; DePaula, R. F.; Zheng, L. X.; Zhao, Y. H.; Stan, L.; Holesinger, T. G.; Arendt, P. N.; Peterson, D. E.; Zhu, Y. T. Sustained Growth of Ultralong Carbon Nanotube Arrays for Fiber Spinning. *Adv. Mater.* **2006**, *18*, 3160–3163.
41. Mizuno, K.; Ishii, J.; Kishida, H.; Hayamizu, Y.; Yasuda, S.; Futaba, D. N.; Yumura, M.; Hata, K. A Black Body Absorber from Vertically Aligned Single-Walled Carbon Nanotubes. *Proc. Natl. Acad. Sci. U. S. A.* **2009**, *106*, 6044–6047.
42. Rao, A. M.; Jorio, A.; Pimenta, M. A.; Dantas, M. S. S.; Saito, R.; Dresselhaus, G.; Dresselhaus, M. S. Polarized Raman Study of Aligned Multiwalled Carbon Nanotubes. *Phys. Rev. Lett.* **2000**, *84*, 1820–1823.
43. Dettlaff-Weglikowska, U.; Skákalová, V.; Graupner, R.; Jhang, S. H.; Kim, B. H.; Lee, H. J.; Ley, L.; Park, Y. W.; Berber, S.; Tománek, D. Effect of Socl2 Treatment on Electrical and Mechanical Properties of Single-Wall Carbon Nanotube Networks. *J. Am. Chem. Soc.* **2005**, *127*, 5125–5131.
44. Wang, S.; Liang, Z.; Wang, B.; Zhang, C. High-Strength and Multifunctional Macroscopic Fabric of Single-Walled Carbon Nanotubes. *Adv. Mater.* **2007**, *19*, 1257–1261.
45. Malik, S.; Rosner, H.; Hennrich, F.; Bottcher, A.; Kappes, M. M.; Beck, T.; Auhorn, M. Failure Mechanism of Free Standing Single-Walled Carbon Nanotube Thin Films under Tensile Load. *Phys. Chem. Chem. Phys.* **2004**, *6*, 3540–3544.
46. Xu, G. H.; Zhang, Q.; Zhou, W. P.; Huang, J. Q.; Wei, F. The Feasibility of Producing MWCNT Paper and Strong Mwcnt Film from VACNT Array. *Appl. Phys. A: Mater.* **2008**, *92*, 531–539.
47. Dikin, D. A.; Stankovich, S.; Zimney, E. J.; Piner, R. D.; Dommett, G. H.; Evmenenko, G.; Nguyen, S. T.; Ruoff, R. S. Preparation and Characterization of Graphene Oxide Paper. *Nature* **2007**, *448*, 457–460.
48. Park, S.; Lee, K. S.; Bozoklu, G.; Cai, W.; Nguyen, S. T.; Ruoff', R. S. Graphene Oxide Papers Modified by Divalent Ions−Enhancing Mechanical Properties Via Chemical Cross-Linking. *ACS Nano* **2008**, *2*, 572–578.
49. Chen, H.; Muller, M. B.; Gilmore, K. J.; Wallace, G. G.; Li, D. Mechanically Strong, Electrically Conductive, and Biocompatible Graphene Paper. *Adv. Mater.* **2008**, *20*, 3557–3561.
50. Borkowski, J. W. Process for Making High Strength Flexible Graphite Foil. U.S. patent 4102960, 1978.
51. Jia, J. J.; Zhao, J. N.; Xu, G.; Di, J. T.; Yong, Z. Z.; Tao, Y. Y.; Fang, C. O.; Zhang, Z. G.; Zhang, X. H.; Zheng, L. X.; *et al.* A Comparison of the Mechanical Properties of Fibers Spun from Different Carbon Nanotubes. *Carbon* **2011**, *49*, 1333–1339.
52. Qian, D.; Liu, W. K.; Ruoff, R. S. Load Transfer Mechanism in Carbon Nanotube Ropes. *Compos. Sci. Technol.* **2003**, *63*, 1561–1569.
53. Qian, D.; Wagner, G. J.; Liu, W. K.; Yu, M. F.; Ruoff, R. S. Mechanics of Carbon Nanotubes. *Appl. Mech. Rev.* **2002**, *55*, 495.
54. Berhan, L.; Yi, Y. B.; Sastry, A. M.; Munoz, E.; Selvidge, M.; Baughman, R. Mechanical Properties of Nanotube Sheets: Alterations in Joint Morphology and Achievable Moduli in Manufacturable Materials. *J. Appl. Phys.* **2004**, *95*, 4335–4345.
55. Peter Chen, I. W.; Liang, R.; Zhao, H.; Wang, B.; Zhang, C. Highly Conductive Carbon Nanotube Buckypapers with Improved Doping Stability Via Conjugational Cross-Linking. *Nanotechnology* **2011**, *22*, 485708.
56. Cheng, Q. F.; Bao, J. W.; Park, J.; Liang, Z. Y.; Zhang, C.; Wang, B. High Mechanical Performance Composite Conductor: Multi-Walled Carbon Nanotube Sheet/Bismaleimide Nanocomposites. *Adv. Funct. Mater.* **2009**, *19*, 3219–3225.
57. Shim, B. S.; Zhu, J.; Jan, E.; Critchley, K.; Ho, S. S.; Podsiadlo, P.; Sun, K.; Kotov, N. A. Multiparameter Structural Optimization of Single-Walled Carbon Nanotube Composites: Toward Record Strength, Stiffness, and Toughness. *ACS Nano* **2009**, *3*, 1711–1722.
58. Liu, W.; Zhang, X. H.; Xu, G.; Bradford, P. D.; Wang, X.; Zhao, H. B.; Zhang, Y. Y.; Jia, Q. X.; Yuan, F. G.; Li, Q. W.; *et al.* Producing Superior Composites by Winding Carbon Nanotubes onto a Mandrel under a Poly(Vinyl Alcohol) Spray. *Carbon* **2011**, *49*, 4786–4791.
59. Di, J.; Yong, Z.; Yang, X.; Li, Q. Structural and Morphological Dependence of Carbon Nanotube Arrays on Catalyst Aggregation. *Appl. Surf. Sci.* **2011**, *258*, 13–18.
60. Toupin, M.; Brousse, T.; Bélanger, D. Charge Storage Mechanism of MnO_2 Electrode Used in Aqueous Electrochemical Capacitor. *Chem. Mater.* **2004**, *16*, 3184–3190.
61. Bélanger, D.; Brousse, T.; Long, J. W. Manganese Oxides: Battery Materials Make the Leap to Electrochemical Capacitors. *Interface-Electrochem. Soc.* **2008**, *17*, 49–52.